INSTITUTO SUPERIOR TÉCNICO
Universidade Técnica de Lisboa

Local/Distorcional Interaction in Hat Section Columns

Rui Fena
Instituto Superior Técnico, Technical University of Lisbon, Lisbon, Portugal
ruitfena@gmail.com

Abstract: The results of an investigation concerning the post-buckling behaviour (elastic and elastic-plastic), ultimate strength and design of fixed-ended cold formed steel hat section columns experiencing local-plate/distorcional buckling mode interaction are presented and discussed. All geometrically and physically nonlinear analyses are carried out in the code Abaqus, discretising the columns into fine shell finite element meshes. The columns analysed (i) have cross-section dimensions leading to similar local and distortional critical buckling stresses, and (ii) contain critical-mode initial geometrical imperfections with various shapes, obtained from different linear combinations of the competing local and distortional modes, and sharing the same amplitude. The numerical results presented consist of (i) elastic and elastic-plastic non-linear (post-buckling) equilibrium paths, (ii) figures describing the evolution, along those equilibrium paths, of the column deformed shapes, and (iii) figures showing the spreading of the plastic strains in the elastic-plastic columns until they reach their ultimate strength values, as well as the characteristics of the corresponding failure modes. Then, one describes the most important results of an extensive parametric study involving the determination of the ultimate strength values of 90 hat section columns with several geometries (cross-section dimensions and length) and yield stresses, carefully chosen to exhibit strong L/D mode interaction – all columns contain the most detrimental critical-mode geometrical imperfections with a small amplitude. Finally, the ultimate strength values obtained in the above parametric study are used to assess the performance of existing Direct Strength Method (DSM) design approaches in predicting local/distortional column interactive failures.

Keywords: cold-formed steel columns, local-plate and distorcional buckling, mode interaction, post-buckling, finite element method, direct strength method

1. Introduction

Most cold-formed steel members have slender thin-walled open cross-sections, which makes them prone to local and distortional buckling. Moreover, since several common cold-formed steel member geometries (cross-section shape /dimensions and unrestrained length) are associated with similar local and distortional buckling stresses, the corresponding post-buckling behaviour, ultimate strength and failure mechanism are likely to be strongly affected by interaction effects involving these two instability phenomena.

A considerable amount of research has been recently devoted to developing efficient (safe and economic) design rules for cold-formed steel members. The most relevant output of this intense activity was the "Direct Strength Method" (DSM), originally proposed by Schafer & Peköz [1] and continuously improved, mostly due to Schafer's efforts (e.g., [2, 3]). The DSM (i) accounts for the combined effect of local, distortional and global buckling, (ii) does not require "effective width" calculations and (iii) was already incorporated in the current versions of the North American and Australian/New Zealander cold-formed steel design specifications. However, as pointed out by Schafer [3], further research is needed before the DSM approach can be applied to members affected by mode interaction phenomena involving distortional buckling.

Concerning the local/distortional interaction, almost all of the available results stem from investigations on cold-formed steel lipped-channel columns or beams (e.g., [4-11]) – note that some of these works already led to the development and calibration of novel DSM design curves [5, 9, 11]. Studies involving members with other cross-section shapes are still very scarce – indeed, to the authors' best knowledge, only rack-section columns were investigated [12]. In particular, there are no available studies on hat-section members.

Therefore, the objective of this paper is to present and discuss numerical results concerning

the post-buckling behaviour and ultimate strength of fixed cold-formed steel hat-section columns affected by local/distortional interaction – the results are obtained through Abaqus shell finite element analyses. To enable a thorough assessment of the mode interaction effects, the column geometries (cross-section dimensions and lengths) are selected to ensure very close local (L) and distortional (D) buckling loads. By analysing members with different yield stresses, it is also possible to assess how the relevance of local/distortional interaction varies with the yield-to-critical stress ratio. Finally, the ultimate strength data gathered are compared with the estimates of the available DSM expressions, including those recently published [9, 11], in order to assess whether they can successfully handle the design of hat-section columns against L/D interactive failures.

2. Local/Distorcional Buckling Mode Interaction

One reports here the main results of a investigation on the elastic-plastic post-buckling behaviour and ultimate strength of fixed hat-section columns strongly affected by local/distortional buckling interaction – the columns analysed (i) have the cross-section dimensions, length and elastic constants indicated in Fig. 1(a) and (ii) buckle elastically for P_{cr}=*90.1 kN* (f_{cr}=*211.5 MPa*) in arbitrary combinations of (ii_1) a *17* half-wave local and (ii_2) a *3* half-wave distortional modes, as illustrated in Fig. 1(b).

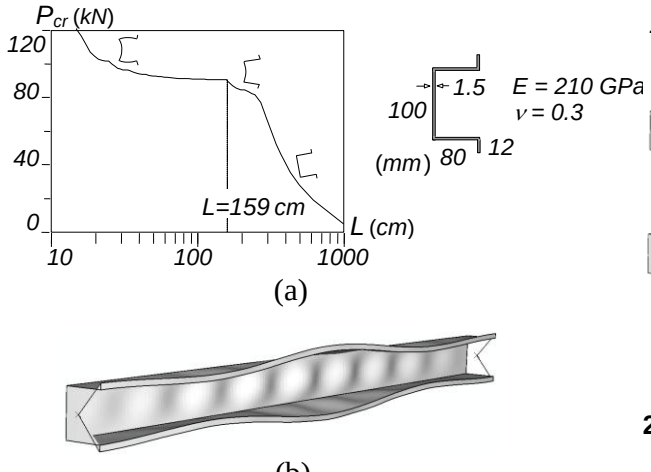

Figure 1 – (a) Column Buckling curve and (b) $L_{L/D}$ column buckling mode shape.

The results were obtained through ABAQUS shell finite element analyses that (i) adopt column discretisations into fine 4-node isoparametric element meshes (length-to-width ratio close to *1*), (ii) model the column supports by attaching rigid plates to the end section centroids and (iii) describe the steel material behaviour by a linear-elastic/perfectly-plastic stress-strain curve (both residual stresses and corner effects are disregarded) – a detailed account of all the column finite element modelling issues can be found in [6].

2.1 Initial Geometrical Imperfections

The initial geometrical imperfection shape always plays a crucial role in mode interaction investigations, as its choice may alter considerably the post-buckling behaviour and strength of the structural system under consideration. Thus, it is necessary to investigate the post-buckling behaviour of members containing various critical-mode initial shapes, combining arbitrarily the two competing L and D buckling modes [6] and sharing the same overall amplitude. In this study, the column initial configurations consist of linear combinations of a *17* half-wave local and a *3* half-wave distortional buckling modes, both normalised to exhibit amplitudes equal to *10%* of the wall thickness *t* (*0.1 t=0.15 mm*). The linear combination coefficients $C_{L.0}$ and $C_{D.0}$ satisfy the condition $(C_{L.0})^2+(C_{D.0})^2=1$, and the initial imperfection is defined by angle θ, such that $C_{L.0}=\sin\theta$ and $D_{D.0}=\cos\theta$ in Fig. 2(a). Fig. 2(b) shows the pure L (θ=*90º* or *270º* – inward/outward mid-span web bending) and D (θ=*0º* or *180º* – inward/outward mid-span flange-stiffener motions) column initial imperfections.

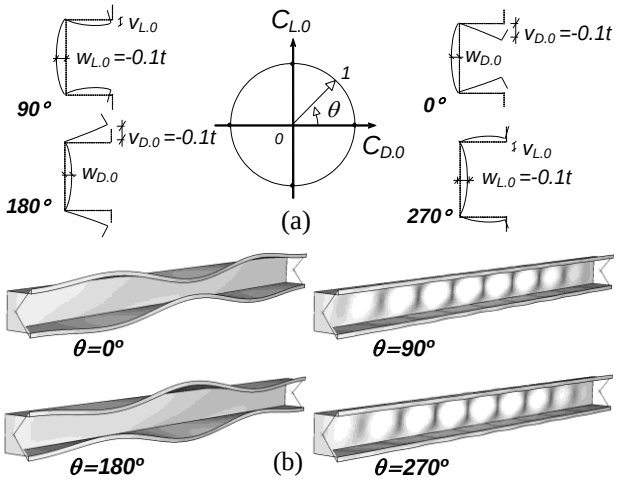

Figure 2 – (a) Initial imperfection representation in the $C_{D.0}$-$C_{L.0}$ plane and (b) initial imperfection shapes for *θ=0º, 90º, 180º* and *270º* hat section columns.

2.2 Elastic-Plastic Post-Buckling Behaviour

The influence of local/distortional interaction in the elastic-plastic post-buckling behaviour is assessed by considering fixed hat-section columns (i) containing *8* initial imperfection shapes, defined by θ=*0º*, *45º*, *90º*, *135º*, *180º*, *225º*, *270º*, *315º*, and (ii) exhibiting *4* yield-to-critical stress ratios, $f_y/f_{cr}\approx$*1.2, 1.7, 2.6* and ∞, corresponding to f_y=*250, 350, 550 MPa* and elastic behaviour (recall that $f_{cr}=f_L=f_D$= *211.5 MPa*). Fig. 3(a) shows (i) the upper portions (P/P_{cr}>*0.6*) of the elastic equilibrium paths P/P_{cr} *vs. v/t*, where *v* is the mid-span flange-lip corner vertical displacement, and (ii) the deformed configurations of the θ=*0º*, *90º* and *180º* columns at advanced post-buckling stages.

After observing these results, it is possible to conclude that:

(i) All equilibrium paths shown in Fig. 3(a) combine (i_1) predominant *3* half-wave distortional deformations with (i_2) *17* half-wave local deformations – see the three deformed configurations also displayed in Fig. 3(a). In particular, the emergence of local deformations in the $\theta=0^o$ and $\theta=180^o$ columns ($C_{L.0}=0$) provides clear evidence of occurrence of L/D buckling interaction.

(ii) While the equilibrium paths associated with null ($\theta=90^o$ and 270^o columns) or positive ($\theta=0^o$, 45^o and 315^o columns) $C_{D.0}$ values correspond to distortional deformations involving *inward* mid-span flange-lip motions, the $\theta=135^o$, 180^o and 225^o columns (negative $C_{D.0}$ values) exhibit *outward* motions.

(iii) The equilibrium paths concerning the (iii_1) $\theta=135^o$ and 180^o, (iii_2) $\theta=45^o$, 90^o and 270^o and (iii_3) $\theta=0^o$ and 315^o columns merge into common curves. Since the $\theta=225^o$ column equilibrium path corresponds to a single curve, it may be said that the set of *8* equilibrium paths "converge" towards one of *4* curves, corresponding to inward (two of them) or outward (the remaining two) mid-span flange-lip motions.

(iv) The existence of the two pairs of "converging curves", described in the previous item, was not observed in the fixed lipped channel columns affected by L/D interaction analysed in [7] – all equilibrium paths merged into two common curves, involving inward (one) or outward (the other) mid-span flange-lip motions. This qualitative difference stems probably from the higher half-wave numbers involved: *3* D and *17* L (hat-section columns), against *2* D and *11* L (lipped channel columns).

(v) The pure distortional initial imperfections with *inward* mid-span flange-lip motions ($\theta=0^o$) are the most *detrimental*, in the sense that the corresponding equilibrium paths lie below all the others (*i.e.*, exhibit lower strengths). Recall that pure *outward* distortional initial imperfections were the most detrimental in lipped channel columns affected by L/D interaction [6, 7].

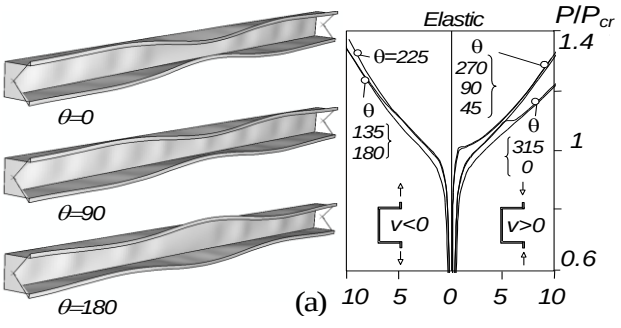

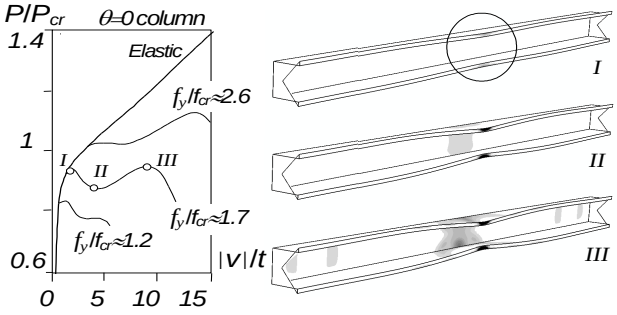

Figure 3 – (a) Elastic P/P_{cr} *vs. v/t* paths + $\theta=0^o$, 90^o and 180^o column deformed shapes, and (b_1) elastic-plastic paths ($\theta=0^o$ + $f_y/f_{cr}\approx1.2, 1.7, 26, \infty$) and ($b_2$) deformed shape and plastic strain evolutions ($\theta=0^o$ + $fy/fcr\approx1.7$).

Fig. 3(b_1) shows the upper portions of four P/P_{cr} *vs. v/t* equilibrium paths of $\theta=0^o$ columns with yield-to-critical stress ratios $f_y/f_{cr}\approx1.2, 1.7, 2.6$ and ∞. Fig. 3(b_2) concerns the column with $f_y/f_{cr}\approx1.7$ and displays three deformed shapes and plastic strain diagrams, associated with the equilibrium states indicated in Fig. 3(b_1) and including the column collapse mode. The observation of these results prompts the following comments:

(i) The onset of yielding, at the mid-span lip free ends (diagram *I* in Fig. 3(b_2)), does not precipitate failure for large enough f_y/f_{cr} values – after the occurrence of a mild "snap-through" phenomenon, the column still exhibits a certain amount of strength reserve (columns with $f_y/f_{cr}\approx1.7, 2.6$).

(ii) For $f_y/f_{cr}\geq1.7$, the collapse occurs after the yielding of the column central regions located in the web and around the web-flange corners – the failure mechanism corresponds to the formation of a "distortional plastic hinge" at mid-span (diagram *III* in Fig. 3(b_2)).

3. Parametric Study: Scope and Numerical Results

Five columns displaying different cross-sections dimensions are used as *reference cases* in this parametric study – they exhibit practically coincident local and distortional critical buckling stresses ($f_{cr}\approx f_L\approx f_D$). In each case, slight variations of the flange (b_f), web (b_w) or stiffener (b_s) width generate two other column sets, exhibiting distinct, but fairly close, f_L and f_D values ($0.90\leq f_L/f_D\leq 1.10$). The above three column sets have cross-section dimensions and lengths identical to those considered in a previous investigation involving fixed lipped channel columns [9]. In order to cover a wide (distortional) slenderness $\lambda=(f_y/f_D)^{0.5}$ range, *5* different yield stresses ($f_y=150$, *250*, *350*, *550*, *750 MPa*) are adopted for each of the *15* columns selected – a total of *75* columns were then analysed. Both the residual stresses (little effect on the cold-formed steel column ultimate strength) and corner effects are neglected in the shell finite element analyses

Table 1 – SFEA ultimate strengths and their DSM estimates (dimensions in mm, stresses in MPA)

				FSA			FEA		DSM												
		L	f_y	L_{crL}	L_{crD}	f_E	f_L	f_D	f_U	λ_D	f_{NL}	f_{ND}	f_{NE}	f_{NLE}	f_{NDL}	f^*_{NDL}	$\frac{f_{NL}}{f_U}$	$\frac{f_{ND}}{f_U}$	$\frac{f_{NDL}}{f_U}$	$\frac{f^*_{NDL}}{f_U}$
b_w =110; b_f=100, t=1.9mm	b_S =17.5	1760	150	105	755	567.4	262.2	262.2	145	0.76	150	136	134	134	136	136	1.03	0.94	0.94	0.94
			250						213	0.98	216	191	208	191	174	191	1.01	0.90	0.82	0.90
			350						245	1.16	270	232	270	227	200	232	1.10	0.95	0.82	0.95
			550						275	1.45	363	296	367	279	237	296	1.32	1.08	0.86	1.08
			750						303	1.69	444	346	431	310	265	284	1.47	1.14	0.87	0.94
	b_S =20	1760	150	100	825	549.7	262.9	284.6	147	0.73	150	139	134	134	139	139	1.02	0.95	0.95	0.95
			250						225	0.94	216	197	207	190	180	197	0.96	0.88	0.80	0.88
			350						274	1.11	270	241	268	226	207	241	0.99	0.88	0.76	0.88
			550						276	1.39	364	308	362	276	246	308	1.32	1.12	0.89	1.12
			750						278	1.62	444	361	424	307	275	275	1.60	1.30	0.99	0.99
	b_S =16	1760	150	105	705	578.7	261.5	243.4	142	0.79	150	134	135	135	134	134	1.06	0.94	0.94	0.94
			250						203	1.01	216	185	209	191	170	185	1.06	0.91	0.84	0.91
			350						223	1.20	270	225	272	228	194	225	1.18	0.99	0.85	0.99
			550						269	1.50	363	286	369	280	229	249	1.35	1.06	0.85	0.93
			750						302	1.76	444	333	436	312	255	283	1.47	1.10	0.85	0.94
b_f =80; b_S=10, t=1.0mm	b_W =95	2500	150	85	595	223.0	103.9	103.9	91	1.20	113	96	113	94	82	96	1.24	1.06	0.90	1.06
			250						111	1.55	157	126	156	116	99	106	1.42	1.13	0.89	0.96
			350						114	1.84	195	149	181	128	111	122	1.71	1.30	0.97	1.07
			550						148	2.30	261	184	196	134	128	145	1.76	1.24	0.87	0.98
			750						157	2.69	317	212	196	134	142	163	2.02	1.35	0.90	1.04
	b_W =88	2500	150	80	585	193.2	114.7	108.2	97	1.18	117	98	108	94	85	98	1.20	1.01	0.87	1.01
			250						115	1.52	163	128	145	114	103	108	1.42	1.12	0.89	0.93
			350						127	1.80	203	152	164	124	115	122	1.59	1.19	0.91	0.96
			550						151	2.25	270	188	169	126	134	145	1.79	1.24	0.88	0.96
			750						165	2.63	329	216	169	126	147	162	1.99	1.31	0.89	0.98
	b_W =105	2500	150	85	595	267.4	89.0	93.0	94	1.27	107	91	119	92	76	91	1.14	0.97	0.81	0.97
			250						103	1.64	149	119	169	116	91	99	1.45	1.16	0.88	0.96
			350						108	1.94	185	140	202	130	102	113	1.71	1.30	0.95	1.05
			550						128	2.43	246	173	233	142	118	135	1.92	1.35	0.92	1.05
			750						152	2.84	299	199	235	143	130	151	1.97	1.31	0.86	1.00
b_f =80; b_S=10, t=1.5mm	b_W =114	1150	150	90	500	1451.2	172.0	172.0	126	0.93	133	119	144	129	110	119	1.06	0.94	0.87	0.94
			250						162	1.21	187	160	233	179	136	160	1.16	0.99	0.84	0.99
			350						190	1.43	234	191	316	219	154	191	1.23	1.01	0.81	1.01
			550						234	1.79	313	240	469	283	180	219	1.34	1.02	0.77	0.94
			750						277	2.09	382	278	604	332	200	251	1.38	1.00	0.72	0.91
	b_W =120	1150	150	100	505	1583.1	157.1	167.5	124	0.95	129	117	144	126	107	117	1.04	0.95	0.86	0.95
			250						158	1.22	182	158	234	174	132	158	1.15	1.00	0.83	1.00
			350						186	1.45	226	189	319	213	150	189	1.22	1.01	0.80	1.01
			550						230	1.81	303	236	476	276	175	222	1.32	1.03	0.76	0.97
			750						262	2.12	369	274	615	325	194	256	1.41	1.05	0.74	0.98
	b_W =106	1150	150	90	495	1277.4	194.4	180.8	128	0.91	139	121	143	134	115	121	1.08	0.94	0.90	0.94
			250						168	1.18	195	163	230	185	142	163	1.16	0.97	0.85	0.97
			350						196	1.39	244	196	312	226	161	196	1.24	1.00	0.82	1.00
			550						241	1.74	327	246	459	291	189	227	1.36	1.02	0.78	0.94
			750						279	2.04	399	285	587	341	210	260	1.43	1.02	0.75	0.93
b_w=100, b_S=10, t=2.4mm	b_f =55	620	150	85	310	3342.1	589.0	590.8	150	0.50	150	150	147	147	150	150	1.00	1.00	1.00	1.00
			250						248	0.65	250	243	242	242	243	243	1.01	0.98	0.98	0.98
			350						341	0.77	350	315	335	335	315	315	1.03	0.92	0.92	0.92
			550						464	0.96	478	424	513	456	389	424	1.03	0.91	0.84	0.91
			750						539	1.13	588	509	683	553	442	509	1.09	0.94	0.82	0.94
	b_f =50	620	150	85	290	3137.1	598.1	625.4	150	0.49	150	150	147	147	150	150	1.00	1.00	1.00	1.00
			250						248	0.63	250	246	242	242	246	246	1.01	0.99	0.99	0.99
			350						343	0.75	350	320	334	334	320	320	1.02	0.93	0.93	0.93
			550						483	0.94	481	434	511	457	398	434	0.99	0.90	0.82	0.90
			750						560	1.10	591	522	679	553	453	522	1.06	0.93	0.81	0.93
	b_f =60	620	150	85	320	3513.5	581.2	558.9	149	0.52	150	150	147	147	150	150	1.01	1.01	1.01	1.01
			250						246	0.67	250	241	243	243	241	241	1.02	0.98	0.98	0.98
			350						333	0.79	350	310	336	336	310	310	1.05	0.93	0.93	0.93
			550						443	0.99	476	415	515	455	380	415	1.07	0.94	0.86	0.94
			750						517	1.16	586	497	686	552	431	497	1.13	0.96	0.83	0.96
b_w=180, b_S=10, t=1.9mm	b_f =110	1030	150	150	590	4401.6	113.1	113.1	104	1.15	116	100	148	115	86	100	1.12	0.96	0.83	0.96
			250						133	1.49	162	131	244	160	104	131	1.22	0.99	0.78	0.99
			350						158	1.76	201	155	339	197	117	155	1.28	0.98	0.74	0.98
			550						198	2.21	269	192	522	260	136	192	1.36	0.97	0.69	0.97
			750						233	2.58	327	222	698	313	150	222	1.40	0.95	0.64	0.95
	b_f =130	1030	150	160	650	4735.7	108.8	100.0	94	1.22	115	95	148	114	81	95	1.22	1.01	0.86	1.01
			250						120	1.58	160	123	245	158	98	123	1.33	1.03	0.82	1.03
			350						143	1.87	199	146	339	195	110	145	1.39	1.02	0.77	1.01
			550						181	2.35	265	180	524	257	127	179	1.46	0.99	0.70	0.99
			750						213	2.74	322	207	702	309	140	206	1.51	0.97	0.66	0.97
	b_f =90	1030	150	145	510	3883.1	116.4	124.3	114	1.10	117	104	148	116	90	104	1.03	0.91	0.79	0.91
			250						147	1.42	164	137	243	199	109	137	1.11	0.93	0.74	0.93
			350						160	1.68	204	163	337	262	123	163	1.27	1.02	0.77	1.02
			550						219	2.10	272	202	518	314	143	202	1.24	0.92	0.65	0.92
			750						254	2.46	331	233	692	692	158	233	1.30	0.92	0.62	0.92

				FSA			FEA			DSM										
		L	f_y	L_{crL}	L_{crD}	f_E	f_L	f_D	f_U	λ_D	f_{NL}	f_{ND}	f_{NE}	f_{NLE}	f_{NDL}	f^*_{NDL}	$\frac{f_{NL}}{f_U}$	$\frac{f_{ND}}{f_U}$	$\frac{f_{NDL}}{f_U}$	$\frac{f^*_{NDL}}{f_U}$
bf =80; bs=12. t=1.5 mm	b_w =100	1590	150	90	555	586.4	211.5	211.5	135	0.84	142	128	135	132	123	128	1.06	0.95	0.91	0.95
			250						185	1.09	201	175	209	178	154	175	1.09	0.95	0.83	0.95
			350						201	1.29	251	211	273	213	175	211	1.25	1.05	0.87	1.05
			550						240	1.61	337	266	371	261	207	236	1.40	1.11	0.86	0.98
			750						271	1.88	411	310	439	291	230	270	1.52	1.14	0.85	1.00
	b_w =105	1590	150	90	560	641	197.7	208.4	133	0.85	139	127	136	130	121	127	1.05	0.96	0.91	0.96
			250						181	1.10	197	174	212	176	151	174	1.09	0.96	0.83	0.96
			350						197	1.30	245	209	278	211	172	209	1.25	1.06	0.87	1.06
			550						241	1.62	329	264	384	261	203	233	1.36	1.10	0.84	0.97
			750						264	1.90	401	308	460	293	225	266	1.52	1.16	0.85	1.01
	b_w =95	1590	150	85	550	1277.4	232.2	215.4	136	0.83	147	128	133	133	127	128	1.08	0.94	0.93	0.94
			250						186	1.08	207	176	205	182	158	176	1.11	0.95	0.85	0.95
			350						206	1.27	259	213	266	216	180	213	1.26	1.03	0.87	1.03
			550						245	1.60	348	269	357	263	212	236	1.42	1.10	0.87	0.96
			750						271	1.87	425	313	416	290	236	269	1.57	1.15	0.87	0.99
																Mean	1.27	1.03	0.84	0.97

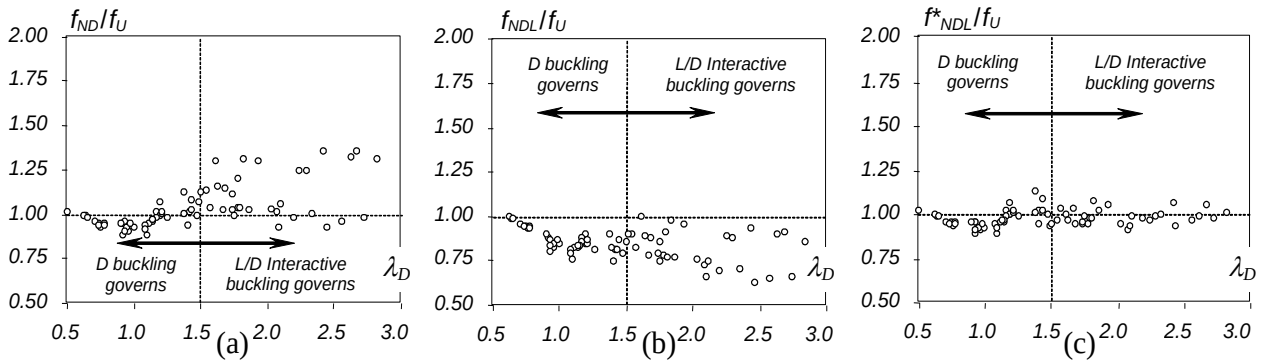

Figure 4 – (a) Variation of (a) f_{ND}/f_U, (b) f_{NDL}/f_U and (c) f^*_{NDL}/f_U with the distorcional slenderness λ_D.

(SFEA) and, regardless of the critical stress ratio f_L/f_D, all columns contained distortional initial geometrical imperfections with (i) inward flange-lip motions of the central half-wave (buckling modes with odd half-wave numbers) and (ii) small amplitude (maximum flange-lip corner displacement equal to *10%* of the wall thickness *t*). All the column cross-section dimensions (b_w, b_f, b_s, t), lengths (L), buckling stresses (f_L, f_D), yield stresses (f_y) and ultimate stresses obtained via SFEA (f_U) are presented in Table 1.

4. Assessment of the DSM estimates

The available DSM applications adopt "Winter-type" design curves, calibrated against fairly large numbers of experimental and/or numerical ultimate strength values. It was shown that, for columns failing in local, distortional or global (flexural or flexural-torsional) modes, it is possible to obtain safe and accurate ultimate strength estimates on the sole basis of elastic buckling and yield stress values – the DSM expressions that prescribe the column *nominal strengths* against *local*, *distortional* and *global* failures (f_{NL}, f_{ND} and f_{NE}) can be found in [3]. Moreover, in order to capture local/global interactive failures, the current DSM approach replaces f_y by f_{NE} in the f_{NL} expressions (f_{NLE} estimates). On the other hand, two distinct strategies were proposed to estimate the ultimate strength of columns experiencing L/D interaction: replacing f_y either (i) by f_{ND} in the f_{NL} equations (NLD approach – f_{NLD}) or (ii) by f_{NL} in the f_{ND} equations (NDL approach – f_{NDL}). Quite recently, Silvestre *et al.* [9] proposed a novel approach to predict more accurately the ultimate strength of fixed lipped channel columns experiencing L/D interaction (f^*_{NDL}), which coincides with f_{ND} for columns with low-to-moderate D slenderness (λ_D *<1.5*). For the more slender columns ($\lambda_D \geq 1.5$), this approach (i) defines a modified local strength f^*_{NL}, which depends on the critical half-wave length ratio L_{crD}/L_{crL}, obtained from the simply supported column "signature curve", and (ii) estimates the column ultimate strength through the replacement of f_{NL} by f^*_{NL} in the NDL equations – these equations leads to f_{ND} and f_{NLD} when $L_{crD}/L_{crL} \leq 4$ and $L_{crD}/L_{crL} \geq 8$, respectively. Table 1 presents the DSM ultimate strength estimates (f_{NL}, f_{ND}, f_{NE}, f_{NLE}, f_{NDL}, f^*_{NDL}) and relevant quantities involved in their calculation, namely the distortional slenderness λ_D and the *simply supported* column distortional and local critical half-wave lengths L_{crD} and L_{crL} (yielded by GBT analyses).

Figs. 4(a)-(c) show the variation of f_{ND}/f_U (Fig. 4(a)), f_{NLD}/f_U (Fig. 4(b)) and f^*_{NDL}/f_U (Fig. 4(c)) with λ_D. The observation of these figures and of the results presented in Table 1 makes it possible to conclude that:

(i) First of all, it should be noted that, for *31* columns, the minimum DSM ultimate strength estimate is f_{NLE}, indicating a local/global interactive failure. Since the visual inspection of

the corresponding SFEA collapse modes showed (i_1) clear evidence of local and distortional deformations, and (i_2) no trace of global deformations, those columns are treated here as failing in local/distortional interactive modes.

(ii) Both f_{NL} and f_{ND} underestimate f_U. The latter are better estimates: f_{ND}/f_U average and standard deviation of *1.03* and *0.12*, with *38* values safe/accurate ($0.90<f_{ND}/f_U\leq 1.00$) and *16* values too unsafe ($f_{ND}/f_U>1.10$).

The f_{ND} error grows with λ_D (see Fig. 4(a)) – the f_{ND} values are accurate and mostly safe for $\lambda_D<1.5$ (no relevant L/D interaction effects), but inaccurate and mostly unsafe for $\lambda_D\geq 1.5$. This means thatthe L/D interaction erodes the column distortional failure load – an erosion not properly predicted by f_{ND}.

(iv) The f_{NDL} estimates are rather conservative and little scattered: f_{NDL}/f_U average and standard deviation of *0.84* and *0.09*, with *18* values safe and accurate, *57* values too safe ($f_{NDL}/f_U\leq 0.90$) and only *1* value a bit unsafe ($1.00<f_{NDL}/f_U\leq 1.10$). A large portion of the too safe estimates occurs for $\lambda_D\geq 1.5$ (see Fig. 4(b)).

(v) The f^*_{NDL} estimates are fairly accurate and also little scattered: f^*_{NDL}/f_U average and standard deviation of *0.97* and *0.05*, with *55* values safe/accurate, *4* values too safe, *14* values a bit unsafe and only *1* value too unsafe (corresponding to $f^*_{NDL}/f_U=1.12$). Figs. 4(a)-(c) clearly show that the f^*_{NDL}/f_U values are much closer to the horizontal line than their f_{ND}/f_U and f_{NDL}/f_U counterparts – note that they coincide with the f_{NDL}/f_U values for $\lambda_D<1.5$.

Finally, Figs. 5(a)-(b) show (i) the variation, with λ_D, of f_U/f_y (white dots) and f^*_{NDL}/f_y (grey dots) and (ii) the DSM "Winter-type curves" providing the f_{NL}/f_y, f_{ND}/f_y and f_{NDL}/f_y values (assuming that $f_L=f_D$). The results displayed in these figures prompt the following comments:

(i) The f_U/f_y values remain quite "aligned" with a "Winter-type curve", exhibiting a reasonably small "vertical dispersion" that grows with λ_D. They lie (i_1) above the f_{ND}/f_y and f_{NDL}/f_y curves (much closer to the former), for $\lambda_D<1.5$, and (i_2) between the D and DL curves, for $\lambda_D\geq 1.5$. Moreover, the distribution of these f_U/f_y values is quite similar to that reported by Silvestre *et al.* [9] for fixed lipped channel columns experiencing L/D interaction and shown in Fig. 6 (*183* columns), thus meaning that the ultimate strengths of hat-section and lipped channel columns with the same geometries are practically identical – recall that the hat-section column geometries analysed here are a subset of those considered in [9].

(ii) The f^*_{NDL}/f_y values are very well "aligned" with the D curve for (ii_1) $\lambda_D<1.5$ (stocky columns) and (ii_2) $\lambda_D\geq 1.5$ (slender columns) with low L_{crD}/L_{crL} ratios (no relevant L/D interaction). However, they lie clearly below that curve for $\lambda_D\geq 1.5$ with moderate-to-high L_{crD}/L_{crL} values (relevant L/D interaction).

(iii) The DSM approach proposed for lipped channel columns [9] also provides accurate and safe ultimate strength estimates for similar hat-section columns affected by L/D interaction – this is just logical, since they share the same f_L, f_D, L_{crL}, L_{crD} values. Further studies are required to confirm the findings reported in this work and also to investigate whether they can be extended to columns built from other profiles.

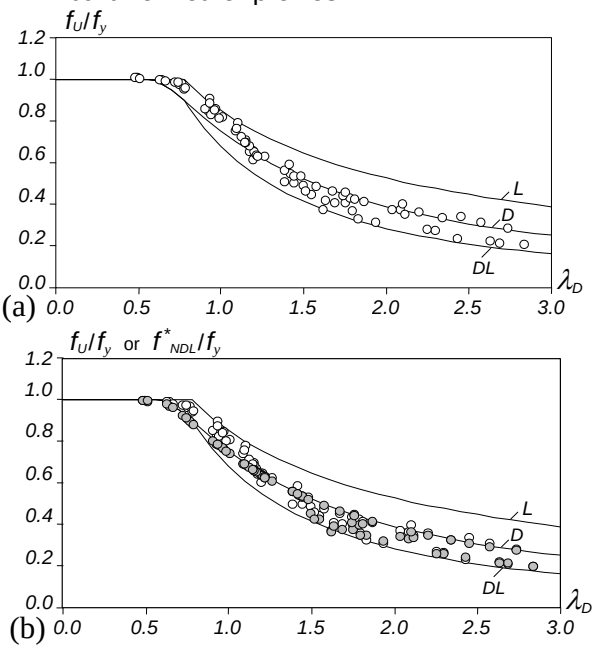

Figure 5 – Variation of (a) f_U/f_y, and (b) f_U/f_y + f^*_{NDL}/f_y with λ_D. for the hat section columns analysed in this work.

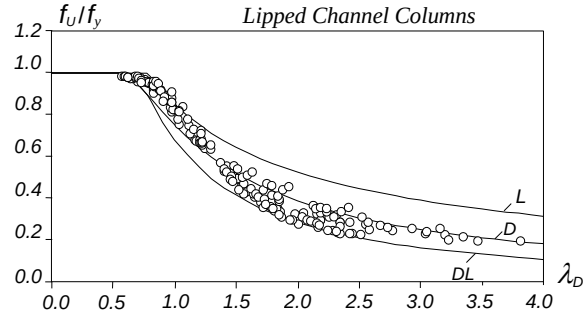

Figure 6 – Variation of f_U/f_y with λ_D. for lipped channel columns analysed by *Silvestre et. al.* [9].

References

[1] Schafer BW, Pekoz T, "Direct strength prediction of cold-formed steel members using numerical elastic buckling solutions", In: *Thin-Walled Structures - Research and Development*, Elsevier, 137-144, 1998.

[2] Schafer BW, *Direct Strength Method Design Guide*. American Iron & Steel Institute, Washington DC, 2005.

[3] Schafer BW, "Review: the direct strength method of cold-formed steel member design", *Journal of Constructional Steel Research*, Vol. 64, No. 7-8, 766-778, 2008.

[4] Ungureanu V, Dubina D, "Recent research advances on ECBL approach – Part I: plastic-elastic interactive buckling of cold-formed steel sections", *Thin-Walled Structures*, Vol. 42, No. 2, 177-194, 2004.

[5] Yang D, Hancock GJ, "Compression tests of high strength steel columns with interaction between local and distortional buckling", *Journal of Structural Engineering* (ASCE), Vol. 130, No. 12, 1954-1963, 2004.

[6] Dinis PB, Camotim D, Silvestre N, "FEM-based analysis of the local-plate/distortional mode interaction in cold-formed steel lipped channel columns", *Computers & Structures*, Vol. 85, No. 19-20, 1461-1474, 2007.

[7] Dinis PB, Young B, Camotim D, "On the effect of local/distortional mode interaction on the post-buckling behaviour and ultimate strength of fixed-ended lipped channel columns", *Proc. IJSSD Symposium on Progress in Structural Stability and Dynamics*, 191-198, Hong Kong, 2009.

[8] Silvestre N, Camotim D, Dinis PB, "Direct strength prediction of lipped channel columns experiencing local-plate/ distortional interaction", *Advanced Steel Construction – an International Journal*, Vol. 5, No. 1, 45-67, 2009.

[9] Silvestre N, Camotim D, Dinis PB, "Local/distortional mode interaction in lipped channel steel columns: post-buckling behaviour, strength and DSM design", *Proc. 5th International Conference on Thin-Walled Structures - Recent Innovations and Developments* (ICTWS 2008), 281-288 (vol. 1), Brisbane, 2008.

[10] Dinis PB, Camotim D, "Local/distortional mode interaction in cold-formed steel lipped channel beams", *Thin-Walled Structures*, Vol. 48, No. 10-11, 771-785, 2010.

[11] Kwon YB, Kim BS, Hancock GJ, "Compression tests of high strength cold-formed steel channels with buckling interaction", *Journal of Constructional Steel Research*, Vol. 65, No. 2, 278-289, 2009.

[12] Silvestre N, Dinis PB, Camotim D, "DSM design of simply supported rack-section columns against local-distortional interactive buckling", *Proc. 5th International Conference on Coupled Instabilities in Metal Structures*, 417-424, Sydney, 2008.